

Article

Power-System Flexibility: A Necessary Complement to Variable Renewable Energy Optimal Capacity Configuration

Denis Juma ^{1,*}, Josiah Munda ^{2,*}  and Charles Kabiri ¹

¹ African Centre of Excellence in Energy for Sustainable Development, College of Science & Technology, University of Rwanda, KN 67 Street Nyarugenge, Kigali P.O. Box 3900, Rwanda; c.kabiri@ur.ac.rw

² Department of Electrical Engineering, Tshwane University of Technology, Pretoria X680-0001, South Africa

* Correspondence: jumawabwire@mmust.ac.ke (D.J.); mundajl@tut.ac.za (J.M.)

Abstract: Comprehending the spatiotemporal complementarity of variable renewable energy (VRE) sources and their supplemental ability to meet electricity demand is a promising move towards broadening their share in the power supply mix without sacrificing either supply security or overall cost efficiency of power system operation. Increasing VRE share into the energy mix has to be followed with measures to manage technical challenges associated with grid operations. Most sub-Saharan countries can be considered ‘greenfield’ due to their relatively low power generation baseline and are more likely to be advantaged in planning their future grids around the idea of integrating high VRE sources into the grid from the outset. An essential measure for achieving this objective entails exploring the possibility of integrating renewable hybrid power plants into the existing hydropower grid, leveraging on existing synergies and benefiting from the use of existing infrastructure and grid connection points. This study evaluates the potential for hybridizing existing hydropower-dominated networks to accommodate solar- and wind-energy sources. The existing synergy is quantified using correlation and energy indicators by evaluating complementarity at daily, monthly and annual intervals. The proposed metric serves as a tool to improve planning on increasing the VRE fraction into the existing systems with the aim to achieve optimal power mixes. In comparison to cases in which the same kind of resource is over-planted while expanding installed capacity, the results demonstrate that wind and solar resources hold a positive degree of complementarity, allowing a greater share of VRE sources into the grid. The study shows that Kenya bears favorable climatic conditions that allow hybrid power plant concepts to be widely explored and scaled up on a large and efficient scale. The results can be applicable in other regions and represent an important contribution to promoting the integration of VRE sources into sub-Saharan power grids.

Keywords: variable renewable energy sources; complementarity; compromise programming; grid integration; power system flexibility



Citation: Juma, D.; Munda, J.; Kabiri, C. Power-System Flexibility: A Necessary Complement to Variable Renewable Energy Optimal Capacity Configuration. *Energies* **2023**, *16*, 7432. <https://doi.org/10.3390/en16217432>

Academic Editor: Abdelali El Aroudi

Received: 21 August 2023

Revised: 17 October 2023

Accepted: 26 October 2023

Published: 3 November 2023



Copyright: © 2023 by the authors. Licensee MDPI, Basel, Switzerland. This article is an open access article distributed under the terms and conditions of the Creative Commons Attribution (CC BY) license (<https://creativecommons.org/licenses/by/4.0/>).

1. Introduction

In today’s power dynamics, renewable energy sources (RES) continue to steadily gain prominence. The key enabler of this growth has majorly been based on subsidies such as feed-in tariffs and have played a crucial role in driving this impressive growth. These measures are designed to combat air pollution by encouraging the substitution of fossil fuels with cleaner energy sources. A global transition holds significant importance due to the fact that energy consumption is the primary contributor to global greenhouse gas (GHG) emissions [1]. Shifting towards greater reliance on renewable energy (RE) sources plays a crucial role in attaining universal access to clean and affordable energy, while also abating greenhouse gas emissions and addressing water scarcity concerns by ceasing freshwater consumption associated with thermal power plants [2,3]. This transition is already underway, with renewable energy accounting for over 27% of global electricity

generation by the end of 2019 [4,5], notably with almost 11% generated from renewable energy technologies, largely from wind and solar.

Africa, particularly its sub-Saharan region, is likely to face a unique set of challenges and opportunities as a result of the global energy transition. Many African countries are likely to undergo extremely high rates of energy demand growth in the near future, driven by a range of factors like rapid population growth, sustained economic development and relatively poor access to basic electricity that many African countries are faced with [6].

With unprecedented cost reductions, solar and wind power are becoming an increasingly attractive option for many African countries to contribute to their growing needs, although most African countries still mostly depend on hydropower and natural gas as the main sources of energy [7,8]. One can think of small-scale approaches, such as solar panels on roofs to run household appliances or street lighting with solar panels and batteries; but also of large-scale, grid-connected solar or wind farms. Recent interest to advance non-hydro renewable energy is already stimulating research efforts such as on grid enhancement, flexible hydropower and battery storage to support variable renewable energy (VRE) in specific case studies in Africa [4,9,10].

One might argue that many sub-Saharan countries can be considered ‘greenfield’ compared to the rest of the world due to their relatively low power generation baseline. Indeed, sub-Saharan countries may be more likely to be advantaged in planning their future grids around the idea of integrating high VRE sources from the outset. Africa’s energy transition may be sluggish unless these efforts are scaled up soon [11].

A number of developed countries appear to be at an advanced stage in planning their transition to renewable energy, but the situation is rather different in many African countries. While there are undoubtedly several examples of best practice, some countries in Africa lack even basic resource assessments of VRE potential, thus hampering their efforts to plan towards the progression to renewable energy dependency [12]. With the advent of RE, researchers continue to explore the possibility of combining different renewable energy sources to improve supply security as well as overall system efficiency. In principle, such an analysis can be conducted for either a specific geographic location or for broader regions such as across countries and continents. Presently, the focus of the research carried out has been on stand-alone systems in underdeveloped nations where connection to the grid has been either unfeasible or prohibitively expensive. Some key studies analyzing the prospects for the transition to renewable energy on the African continent are discussed in the following paragraphs.

Utilizing a least-cost optimization model, Barasa et al. [13] assert that greatly expanded VRE, battery storage, and power-to-gas, along with biomass and flexible hydropower, may entirely meet the region’s energy needs at a cheap cost by 2030. Oyewo et al. [10] examined the model results for a cost-optimized power systems in West Africa, reaching a conclusion that by 2050 it would favor a broad adoption of solar PV systems paired with storage across the entire West African region complemented by biomass, wind and the existing hydropower.

A study conducted in [14] presents various scenarios for the expansion of Variable Renewable Energy (VRE) in Eastern and Southern African countries. The study highlights the enormous potential on how improving solar, wind and hydropower and interconnections would significantly reduce greenhouse gas emissions from electricity generation by 2030. Similarly, ref. [15] analyzes the potential of solar PV, wind and Concentrated Solar Power (CSP), emphasizing the importance of international interconnections in expanding VRE capacity and adopting cost-optimal electricity systems. As for South Africa, ref. [16] investigates approaches to shift the country’s electricity generation away from coal by 2050. The study highlights the critical role of photovoltaic, wind and battery storage for daily energy storage and power-to-gas technologies for seasonal power balance.

In addition to the Southern African context, ref. [16] also analyzes the decarbonization options for the North African region’s electricity network by 2030. Their findings align with the South African scenario, emphasizing the significance of solar PV and wind power,

along with battery storage and potential contributions from power-to-gas technology to cater for industrial energy demands. This indicates that the adoption of VRE is crucial for Africa's electricity systems to successfully transition to renewable energy sources. However, according to [11], the current policies in place suggest that VRE will constitute less than 10 percent of Africa's electricity mix by 2030. This prognosis strengthens the position of renewables relative to fossil fuels and raises concerns about the risks of carbon lock-in unless immediate steps are taken to phase out planned fossil fuel power plants.

One of the practical approaches to address the limitations of individual VRE sources is through the integration of multiple sources that complement each other. This concept, known as energetic complementarity, is often quantified using a complementarity index. Complementarity refers to the synergy between energy sources to minimize power output fluctuations on spatial, temporal, or spatio-temporal scales, ensuring energy security. Hybrid renewable energy systems that exploit complementarities between VRE sources may exhibit system reliability and efficiency with less need of energy storage facilities as compared to those based solely on a single energy source.

Due to their weather- and climate-dependent nature, VRE point to unpredictable potential deterring national policymakers and utility companies from considering them as viable alternatives to fossil-fuel-based power generation. For this reason, it is of great importance that weather and climate characteristics targeted at the power generation sector in Africa are put in place. The characteristics of VRE on the African continent may be better mapped out and integrated in power system models. Unfortunately, such services for Africa are in short supply [17]. This hampers the scientific depth of assessments whose main conclusions are centered around strong VRE expansion and increased interconnections. Notably, renewable resource profiles and their mutual synergies and complementarities have not been studied in detail for the African continent, although understanding these is crucial for power systems modeling.

Therefore, with sound conditions, a hybrid system consisting of solar PV, wind, and hydropower could be a good candidate for the region, provided that solar PV and wind power complement each other effectively on diurnal as well as annual scales without requiring significant flexibility options, and when the system's daily and seasonal variability remains low. There is scarce literature that attempts to quantify the synergy between RE resources in East Africa. The current data on RE potential are primarily limited to annual average resource availabilities [18–22]. Solar/wind power mixes have also received much attention lately, although estimates for East Africa remain scanty [23].

Away from Africa, similar research has been conducted across the globe. Without taking into account the local demand profiles, [24] explores how different regions around the world can benefit from supply side complementarity using the stability coefficient defined in [25]. In [26], an optimization model is formulated to find the most optimal placement of wind and PV power plants for achieving an independent power system. This approach is exemplified through a case study in Serbia, showcasing the long-term planning for the complete decarbonization of electricity generation using renewable energy sources. The model presented in [27] utilizes a generation expansion planning approach that incorporates unit commitment and clustered representative days is employed to investigate the most optimal decarbonization strategies for the United Kingdom. The study by [28] analyzes an optimal energy mix planning model for the Korean power system, taking into account the government's support for renewable energy through a renewable portfolio standard (RPS). Meanwhile, [29] investigates various energy and climate change policy scenarios using a comprehensive long-range energy alternatives planning model to determine the optimal power generation structure in South Korea. The study conducted by [30] investigates the efficiency of cost-effective policy incentives in achieving an optimal energy balance in Japan with a primary goal of minimizing the nation's dependence on nuclear power generation. The study utilizes a recursive computable general equilibrium model, coupled with renewable energy input–output tables as an analytical tool. Finally, ref. [31] delves into the intricacies of a well-planned transition towards a zero-emissions

pathway for Chile's electricity system by focusing on capacity expansion and operations to outline an optimal strategy using the ETEM (Energy Technology Environment Model).

With the growing presence of VRE sources in a power system, the operations of the system become more intricate and sophisticated [32]. This is due to the gradual integration of VRE, which introduces greater unpredictability and variability into the net load. The net load profile is an important system characteristic as it enables the extraction of vital information for long-term power system design, particularly for power systems with high VRE shares. Examining the net load profile across different combinations of variable renewable energy sources is a vital undertaking in order to effectively plan for system flexibility as it provides valuable insight on the capability of meeting the load demand by dispatchable generators [33]. This work strives to go beyond the existing averages by introducing a new metric for measuring the synergy between solar PV and wind power potential for hybrid systems on diurnal and seasonal scales, and highlighting its relevance for East Africa's settings with its hydropower dominance. The approach utilizes the system power generation flexibility by first assessing the synergies between the three RES (wind, solar and hydropower) before the hybrid mixes of VREs can be 'tuned' to effectively meet the local demand based on the share index. The metric proposed provides a clear framework for determining the ideal combination of solar and wind power mix to coherently model the transition towards renewable energy.

This article is organized as follows: Section 2 introduces the system model formulation and input assumptions. Section 3 provides an in-depth discussion of the case study area. The results obtained from simulations on the case study and a comparison analysis are presented in Section 4. Finally, Section 5 draws the conclusion and provides remarks for future work.

2. Model Formulation: Algorithm and Input Assumptions

Wind, hydro, and solar power plants and the related space-time features were selected as the focus of the study.

Diurnal, monthly and annual time scales are utilized to examine the complementary characteristics. To quantify the overall level of complementarity, a multidimensional complementary index is constructed using a space vector approach. Figure 1 illustrates the study's framework and structure. The proposed metric serves as a tool to improve planning on increasing the VRE fraction into the existing systems with the aim to achieve optimal power mixes.

East Africa is set to continue its growth, with the population expected to increase by 25% by 2030, and economic growth following suit. This study assumes that the narrative demographic and economic factors lead to a rise in demand for energy, which is consistent with the current trend in the region [7]. In an effort to lessen GHG emissions, investments in power grids would result in huge growth in solar and wind energy use. Synergies of wind-solar-hydro potential for several scenarios of meeting the electricity demand are considered. For each case, different shares of solar and wind power generation are studied that may minimize the residual demand which would basically be supplied by backup generation, potentially at significant monetary and carbon costs.

In the reference case (current demand with no solar and wind generation), the energy demand is met largely by hydropower generation and additional backup to fulfill residual demand imported from the wider grid network (Figure 1). For the sake of simplicity, the electrical demand time series is normalized (i.e., hourly average demand = 1). Power generation time series are also normalized relative to the average demand of the initial case. The rest of the analysis is carried out by varying the normalised contribution from wind and solar power sources to attain the optimal mix.

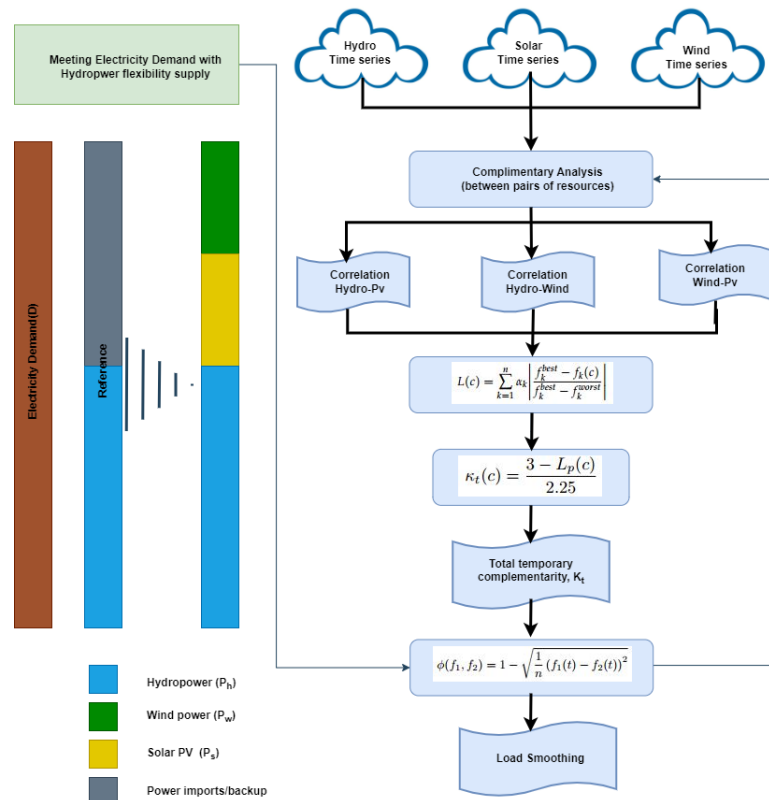


Figure 1. Flow chart of the adopted analytical framework.

2.1. Complementary Characteristics by Means of the Correlation Coefficients

Kendall Tau correlation coefficient is a correlation measure that takes into account the rank of random variables. It indicates the presence of monotonic correlations between variables, capturing the consistency of changing trends [34–36].

The premise of consistency underlies the tenets of Kendall’s tau. If (x_j, y_j) and (x_k, y_k) are two elements of a sample $\{(x_i, y_i)\}_{i=1}^n$ from a bivariate population, one affirms that (x_i, y_i) and (x_j, y_j) are consistent if $(x_i - x_j)(y_i - y_j) > 0$, otherwise inconsistent when $(x_i - x_j)(y_i - y_j) < 0$.

There are $\binom{n}{2}$ distinct pairs of observations in the sample, and each pair (excepting ties) is either consistent or inconsistent. Denoting K for the number of consistent pairs (c) minus the number of inconsistent pairs (d), then the Kendall tau correlation coefficient for the reference sample can be defined as follows:

$$\tau = \frac{c - d}{c + d} = \frac{K}{\binom{n}{2}} = \frac{2K}{n(n - 1)} \tag{1}$$

$$K = \sum_{i=1}^{n-1} \sum_{j=i+1}^n \zeta(x_i, x_j, y_i, y_j),$$

$$\zeta(x_i, x_j, y_i, y_j) = \begin{cases} 1 & \text{if } (x_i - x_j)(y_i - y_j) > 0 \\ 0 & \text{if } (x_i - x_j)(y_i - y_j) = 0 \\ -1 & \text{if } (x_i - x_j)(y_i - y_j) < 0 \end{cases}$$

The correlation coefficient is a measure that usually varies between -1 and $+1$. Values close to zero signify little or no correlation between the matched sets of variables. A positive correlation coefficient suggests that a decrease or increase in one set of variables coincides

with a similar decrease or increase in the other set of variables. Conversely, a negative correlation means that as one set of variables increases, the other set of variables decreases, and vice versa. Table 1, extracted from the study by Canales [37], illustrates the relationship between energy complementarity and correlation coefficient values.

Table 1. Implications of the correlation coefficient level.

Property	Correlation Coefficient Range	Implication
Similarity	0.9 to 1.0	Very strong
	0.6 to 0.9	Strong
	0.3 to 0.6	Moderate
	0.0 to 0.3	Weak
Complementary	−0.9 to 1.0	Very strong
	−0.6 to −0.9	Strong
	−0.3 to −0.6	Moderate
	0.0 to −0.3	Weak

With such an integrated energy system, the output fluctuation can effectively be reduced and stability maintained by its complimentary operation mode.

2.2. Space-Vector-Based Multidimensional Complementary Index

A 3D complementary vector, denoted as c , is designed to capture the complementarity of solar and wind alongside hydropower. The vector, formulated systematically, reflects the correlation between each set of the paired energy sources. Equation (2) illustrates the three terms within the three-dimensional complementary vector, representing the correlation coefficients or complementarity between the energy sources. The Kendall Tau correlation method was employed to calculate each of these correlation coefficients (CC).

$$c = \hat{w}s \cdot CC_{ws} + \hat{w}h \cdot CC_{wh} + \hat{s}h \cdot CC_{sh} \quad (2)$$

Here, solar PV is denoted by s , wind power by w , while h indicates hydropower. Similarly, ws , wh and sh denote wind–solar PV power complementary vector, wind–hydro power complementary vector and solar PV–hydropower complementary vector, respectively. Figure 2 explains vector c representation in 3D space.

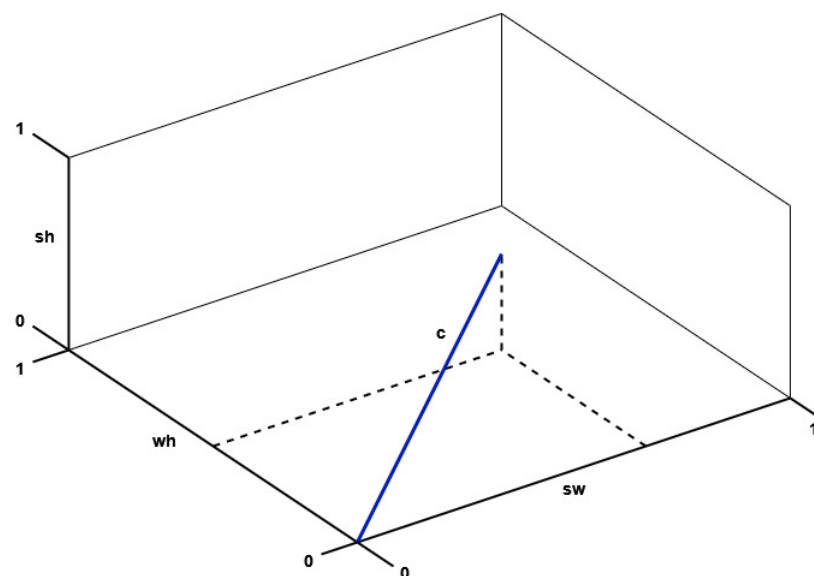


Figure 2. Wind–photovoltaic–hydropower complementary space vector.

The 3D complementary properties of energy combinations allows us to simultaneously measure the degree of complementarity of each pair of energy combinations. However, this 3D vector can only show the extent to which the two energy sources complement one another. Further analysis is therefore required as the complementary properties of the three energy sources cannot be analyzed simultaneously.

In this article, we choose a compromise programming algorithm to further process 3D vector data [38]. This algorithm is utilised to compute the distance between each 3D vector solution as well as the optimal solution to finally determine the total complementary index of the considered three energy sources. Equation (3) below provides the formula for evaluating the best possible solution from the 3D vector space [39,40].

$$L(c) = \sum_{k=1}^n \alpha_k \left| \frac{f_k^{best} - f_k(c)}{f_k^{best} - f_k^{worst}} \right| \tag{3}$$

whereby α_k symbolize the weight of each component in Equation (2) while k denotes each group of complementary energy. f_k is the CC term corresponding to the respective paired energy sources in vector c as captured in Equation (2). $f_k^{best} (= -1)$ is the value of the optimal function in the 3D vector space, signifying total complementarity while $f_k^{worst} (= 1)$ is the worst value denoting null complementarity. According to the proposed method each group of complementary energy is assumed to be of equal weight, thus, $\alpha_k = 1$.

Equation (3) demonstrates that the value of $L(c)$ reaches its theoretical maximum of 1 when the correlation coefficient equals 1. In this scenario, the two energy sources are perfectly correlated, meaning they have identical output curves. This ideal condition can potentially be achieved in practice, making the actual maximum value of $L(c)$ also equal to 1.

The minimum value of $L(c)$ is theoretically 0, when the correlation coefficient equals -1 . This means that the two energy sources are completely complementary, which is not practical. Hence, the actual minimum value of $L(c)$ needs to be determined.

$$\text{Minimize } L(c) = \sum_{k=1}^n \alpha_k \left| \frac{f_k^{best} - f_k(c)}{f_k^{best} - f_k^{worst}} \right| \tag{4}$$

The objective function, $\text{Minimize } L(c)$, aims to identify the optimal minimum value of $L(c)$ within the feasible range. This function can be redefined as the search for the minimum value of $f_k(c)$, which represents the correlation coefficient between various energy sources. Consequently, the minimal value of the correlation coefficient is established.

The correlation coefficient, in the realm of mathematical calculations, acts as a normalization of covariance, effectively simplifying the process into a variance calculation. Suppose we have n variables, denoted as x_i , hence the sum of their variances can be expressed as follows:

$$\begin{aligned} \text{var}(\sum_{i=1}^n x_i) &= \sum_{i,j=1}^n \text{cov}(x_i x_j) \\ &= \sum_{i,j=1}^n \text{cov}(x_i x_j) + \sum_{i \neq j} \text{cov}(x_i x_j) \\ &= n + \sum_{i,j=1}^n \rho_{ij} \\ &= n + \frac{2n!}{2(n-2)!} \bar{\rho} \\ &= n + n(n-1)\bar{\rho} \end{aligned} \tag{5}$$

With $\text{var}(\sum_{i=1}^n x_i) \geq 0$; we have $\bar{\rho} \geq -\frac{1}{n-1}$ (resulting to -0.5 for the case of $n = 3$).

From Equation (4), it is clear that $L(c)$ reaches its minimum value of 0, indicating perfect complementarity. However, when utilizing heuristics and linear programming with three energy sources, the minimum achievable $L(c)$ is 0.75. This can be exemplified when each correlation coefficient of each paired combination is -0.5 [37]. Hence, it can be confidently stated that even with a moderate correlation between two paired VRES, it is still possible to achieve a 100% renewable energy powered system. The addition of a

third energy source can compensate for any shortfalls and minimize the reliance on backup power.

The overall complementarity index, $k_t(c)$ of the three sources may be evaluated by normalizing the value of $L(c)$:

$$k_t(c) = \frac{3 - L(c)}{2.25} \quad (6)$$

and $\kappa_t(c)$ values varying from 0 denoting perfect similarity up to 1 indicating perfect complementarity. The appendix in Canales et al. [37] clearly illustrates and derives the expression for compromise programming as applied in optimising the complementarity between three VRES. Perfect similarity and perfect complementarity is illustrated in Figure 3.

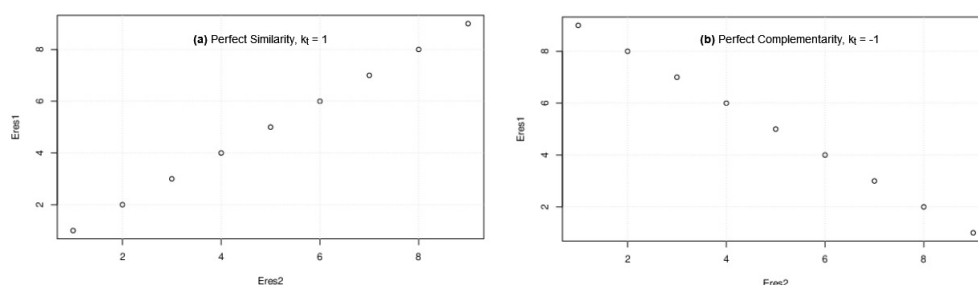


Figure 3. The relationship between paired energy resources; (a) perfect similarity and (b) perfect complementarity.

2.3. Load Smoothing through Complementarity

There exist several criteria of integrating diverse RE sources into the power system. Power output smoothing [41], maintenance of supply–demand balance [42], as well as the system costs reduction [43,44] are a few examples of how combining diverse RE sources may be of benefit to power networks. These approaches are often inter-related; for instance, smoothing out of the generated electric power means reduced variability and shocks, which reduces the necessity for storage hence lowering system costs [45].

To evaluate the smoothness of hybrid power output, numerous studies employ statistical measures. These measures include correlation coefficients between power outputs from different resources, as well as variations in energy balance shapes with an assumption that annual average energy production equals average demand [46,47]. Such techniques have been useful in identifying synergy between renewable resources in diverse areas. However, when implemented across different timescales, they may result in a number of shortcomings as illustrated in Figure 4, such as:

1. Locations with complementary resources are often scored highly even when the strength of the actual resource is too weak for practical exploitation.
2. Resources which may be less complementary and yet strong enough to be useful are often undervalued.

This study seeks to address these problems by introducing a new metric, the optimal share coefficient k_{stab} , as a tool for improving the operation and planning of existing power grids. The metric measures the decrease in the coefficient of variance of the CF of a hybrid w-s-h system with hydro as the baseline while solar and wind carry equal weight. The metric gives the influence of either wind or solar to balance the electric power generation. Stability coefficient, ϕ_s , is mathematically defined as expressed in the Equation below:

$$\phi_s = 1 - \sqrt{\frac{1}{n} \sum_{k=1}^{n-1} (CF_{mix}(t) - CF_{s,w}(t))^2} \quad (7)$$

where, $CF_{mix} = \{\gamma \cdot CF_h + (1 - \gamma)(CF_s + CF_w)/2\}$, the notation CF represents the average capacity factor during the time step t , which is measured hourly. The subscripts s, w, and mix, respectively, represent solar, wind, and hybrid mix. From the expression, ϕ_s varies from 0 to 1, with $\phi_s = 0$, indicating that a unit addition of the considered resource into the hybrid system does not improve the output supply balancing in respect to meeting the expected demand. $\phi_s = 1$ on the other hand means a unit addition of the considered resource to the w-h-s hybrid system carries a bigger impact towards sustaining a constant power output over time hence perfecting the synergy.

With solar–wind contributing to the hybrid system at a ratio of n:m, the expression $n + m = 1 - \gamma$ holds, hence the optimal share coefficient, $k_{stab(s,w)}$ is given as in Equation (8). This evaluates the optimal ratio that each resource has to optimally carry on the power mix while maintaining a balance between the power output and demand profile.

$$k_{stab(s)} = \frac{\phi_s}{\phi_s + \phi_w} \times 100\% \text{ and } k_{stab(w)} = \frac{\phi_w}{\phi_s + \phi_w} \times 100\% \tag{8}$$

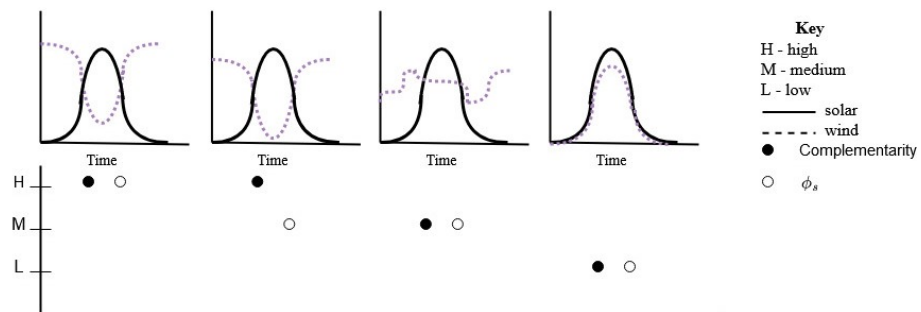


Figure 4. Schematic representation of the variability of stability coefficient with power output of a hybrid system.

A measure of regularity and measure of complementarity are inextricably interlinked. Analysis of a function’s total variation is a typical method of measuring its regularity. One common approach of quantifying regularity of a function is by using its overall variation, which accounts for discontinuities. Studies by Cantor and Daina [48,49], on time series analysis, have explored the concept of total variation. This new metric is anchored on this concept.

This study calculates the stability factor, k_{stab} , for solar and wind capacity installed at the same location. Furthermore, it is possible to expand the analysis to encompass the potential synergies between power stations situated in various regions, taking into account the transmission factor. The coefficient gives the relative share of solar and wind that yields improved output taking into account hydropower as the baseline. This ensures that the installed output exhibits a similar complementarity characteristics as that of the considered timescales.

2.4. Power Generation Modeling

(i) Hydropower Model

The estimation of hydropower generation is determined using the following equation:

$$P_{HP} = Q(t) \cdot H \cdot \zeta \cdot \rho \cdot g \tag{9}$$

where $Q(t)$ represents the river flow rate or water release from the reservoir; H denotes the reservoir elevation. ζ , ρ and g are constants that, respectively, represent the system efficiency, water density, and gravitational acceleration.

(ii) Solar PV Model

Equation (8) illustrates the solar power generation [50]:

$$P_{pv} = \sum BI(t, i) \{1 - \mu(T_a(t, i) - T_c) - \mu CL(t, i)\} \quad (10)$$

where I (W/m^2) is the effective solar irradiance registered at an optimal tilt and estimated using the method described in [51]. The air temperature, T_a ($^{\circ}C$), impacts the performance of the solar panel efficiency. B represents the constant power generation parameter calculated as the product of the PV array area (in square meters) and the efficiency of the generator and inverter (expressed as percentages). μ and C are temperature and radiation dependent efficiency loss factors, respectively, while T_c corresponds to the PV cell temperature under standard test conditions.

(iii) Wind Power Model

To estimate the wind power generation at a specific hour (t), we rely on the wind speed as a determining factor. This estimation uses a modified power curve for a typical wind turbine with the following specifications: a power rating of 1 kW, a cut-in wind speed of 2.5 m/s and a cut-out wind speed of 25 m/s. This allows estimation of the power generation based on the hourly average wind speeds [52] as shown in Equation (11) below.

$$P_w(v, t) = p_1 + \frac{v - v_1}{v_2 - v_1} (p_2 - p_1) \quad (11)$$

with P_w the hourly wind power generation.

(iv) Normalized generation configuration

Power generation from wind, solar and hydro is normalized using the following approach:

$$P^*(t) = \frac{P(t)}{P} \quad (12)$$

where, P^* is the normalized power at time t , P is amount of power produced at time t , estimated using the relevant model according to Equations (9)–(11) while P is the nominal generating capacity of the plant under consideration.

At any given electricity demand case, the total output power generation from the system is captured as:

$$P_{tot}^* = C_{hp}P_{hp} + C_wP_w + C_{pv}P_{pv} + \Delta R \quad (13)$$

Here, P_{hp} , P_w and P_{pv} denotes power generation from hydro, wind and solar energy sources, while C_{hp} , C_{pv} and C_w are the weights corresponding to the contribution of each energy source. ΔR is the residual power not met by the considered sources.

3. Case Study and Datasets

3.1. Kenyan Electricity Sector

Kenya is a country in eastern Africa, bisected by the equator, with a 470 km-long coastline and a diversified topography that rises to 5199 m above sea level. As of 2015, it had a population of about 46 million people up from 31 million back in 2000. With a GDP increase from USD 12.7 billion in 2000 to USD 63.4 billion in 2015, the economy has been growing steadily. In 2017, only 60% of Kenya's population had access to electricity, with only about 20 percent in the rural areas, although this situation is swiftly changing. This increase necessitates diversification of electrical energy options.

The trend in electricity generation has steadily been rising over the years to meet demand. Wind electricity generation rose sixteen-fold over the five-year period with more injection into the grid of Kipeto Wind Power plant in 2021. Similarly, solar electricity generation increased significantly with the addition of Selenkei, Cedate and Malindi power plants to the grid in the same period. On the other hand, both geothermal and hydro electricity generation have taken a downward trajectory in 2021. Just like other sub-Saharan

countries, the trend indicates the concerted effort of harnessing VRE into the existing energy mix.

3.2. The Turkwel River Basin

Figures 5 and 6 depicts the characteristics of the study area. The Turkwel River basin, situated in north-western Kenya, serves as the chosen case study area. The river springs on Mount Elgon on the Ugandan side and flows into Lake Turkana, world biggest desert lake [53,54], spanning an extensive catchment area of approximately 24,000 sq. km. The basin exhibits a distinctive south-west to north-east rainfall gradient with an intertwined hydroclimate amid an extremely diversified terrain. The northern lowland plains of the basin experience a dry climate, with annual rainfall of 99 to 400 mm/year. In contrast, the southern highlands receive higher precipitation levels, ranging between 900 and 1749 mm/year. The basin has two main rainy seasons: a prolonged period from March to June and a sporadic rainy period from October to December.

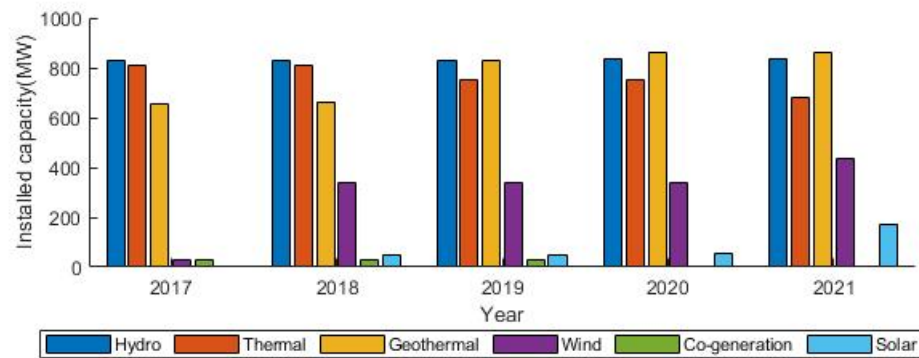


Figure 5. Installed capacity.

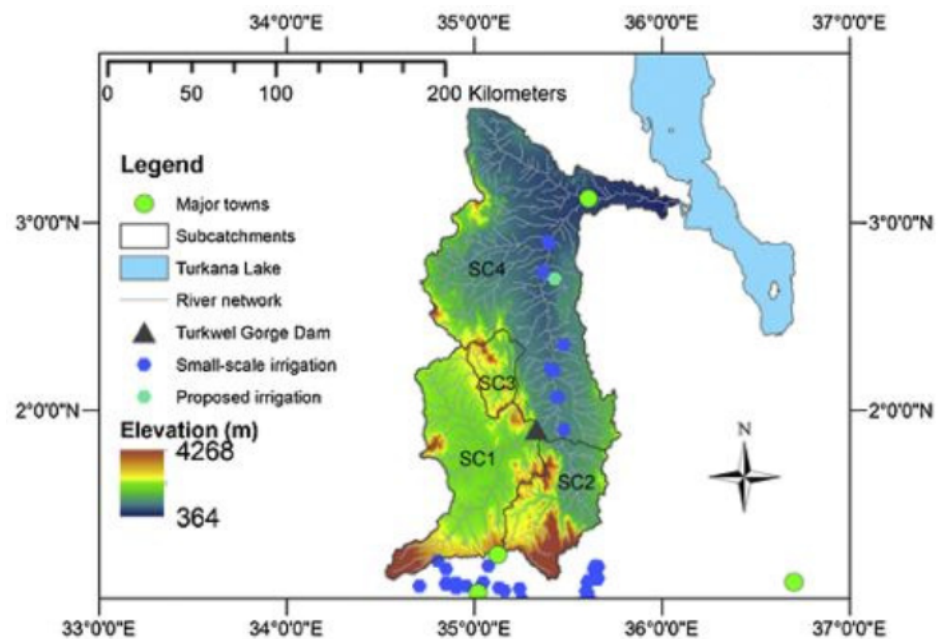


Figure 6. The Turkwel River Basin with four sub-basins based on climatic condition, topography and land cover. Lodwar town is located at the lower end of the basin.

The produced energy output is essentially dependent on stream discharge and is considered to be proportionate to river flow, making it vulnerable to its variability.

As discussed, the proposed method explores flexibility in power generation to realize the benefits of system-wide complementarity. A series of compromises have been applied to profoundly demonstrate this in depth.

3.3. Wind and Solar Time Series

Data sets from Renewables.ninja, an open data source published by ETH Zürich and Imperial College London [55,56] are utilised. It can be accessed either as pre-computed data sets or via an API for particular locations with the option of specifying energy production technology details.

We utilize aggregate capacity factors modeled using the Renewables.ninja model to measure the power generation capability. CF is generation normalized by installed capacity and can be exemplified as the potential for generation with equal installed capacities. Beyond technology and site-specific limits, CF for wind and solar PV is quite sensitive to weather conditions [57].

In this case, the capacity factor of the solar cells is estimated by modeling the efficiency of monocrystalline silicon cells as a function of global horizontal irradiation (GHI) G and air temperature T , following the approach described [51]. On the same note, the capacity factor of wind turbines is modeled based on the method presented in [52]. This model considers the hub-height wind speed and is specifically anchored on Vestas V126-3.3 with 80 m hub height and 3.3 MW rated power, similar to those employed at the Lake Turkana Wind Power project (LTWP), a major wind power project in Africa located in northern Kenya [58].

Figure 7 shows the CF for solar and wind across the region with 0.15 as the lowest registered value. On average, the wind potential is considerable, with CF increasing northwards, reaching 0.40–0.50 over most of the case area. This observation that is supported by the findings of a study of four sites within the study area by [59,60], demonstrates that they are quite feasible for exploitation. Solar energy potential is lower and more concentrated towards the north, with significant region exhibiting CF of 0.15 or higher.

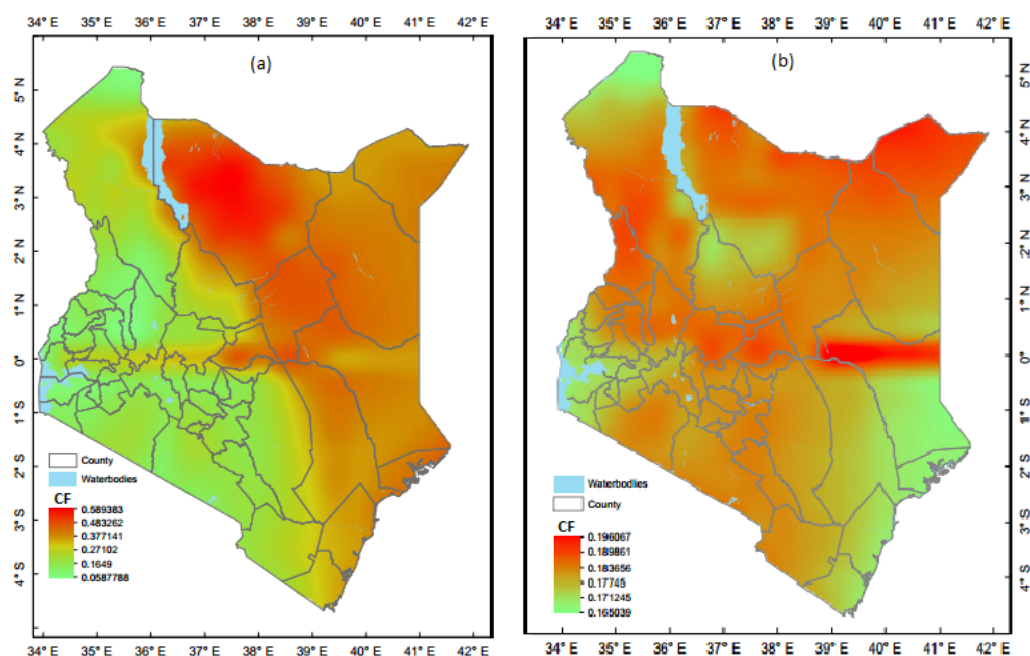


Figure 7. The average annual capacity factors of solar photovoltaic (PV) and wind power, calculated over a five-year time scale (2015–2019). (a) for solar photovoltaic and (b) for wind power.

3.4. Power System Flexibility

To effectively manage the growing integration of variable renewable energy sources, it is crucial to harness flexibility across all sectors of the energy system [32,61,62]. Figure 8 depicts how the entire network, encompassing power generation, transmission, distribution systems, storage (both electrical and thermal), and flexible demand, works together as a unified system.

In conventional power systems, generation has traditionally been the primary source of flexibility, with dispatchable generators altering their output to follow demand and, if available, pumped hydro servicing inflexible baseload and lowering the requirement for power plants to meet peak demand. In recent years, significant effort has been made in increasing the flexibility of conventional power plants, whereas the demand side has generally been unresponsive, offering very little flexibility [63,64]. Emerging technologies are not only boosting supply side flexibility, but they are also broadening space throughout every facet of the power system, such as the grids and the demand side. This initiative offers a broader portfolio of solutions that can be combined and optimized to cut on operational costs alongside other benefits.

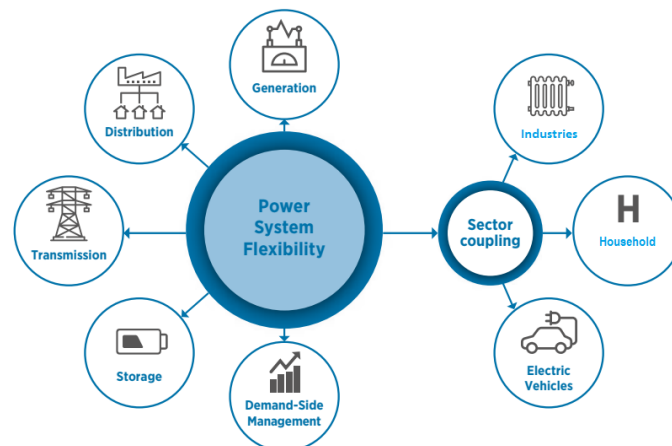


Figure 8. Key drivers for enhancing power system flexibility in the energy sector.

As observed in many regions, there are several efficient ways to incorporate renewables at minimal cost by developing operational procedures as well as a responsive electrical energy market. At some stage during the transition, more capital-intensive measures will be needed. These experiences have also shown that if the appropriate measures are put in place, difficulties associated with VRE integration such as rising curtailment levels and reserve requirements can be managed.

This study aims to reinforce the need for synergistic operation of hydropower and VRE with the aim of taking advantage of natural seasonal variations in the outflows of the multi-year water reservoirs with the aim of dispatching hydropower during periods of low VRE generation hence harnessing the attributes complementarity from the harvested energy sources.

4. Results and Discussion

This section adopts normalised sets of installed capacity for wind, solar and hydropower. The considered power stations are located in the north-west part of Kenya to evaluate the spatial-temporal impact on their complementarity based on yearly, monthly, and daily time scales for the analysis. The wind, solar PV and hydropower generation data in the three time scales is substituted into Equation (2) to generate a 3D vector formula. Using Equations (3) and (4), the optimal solution, $k_t(c)$, of the 3D space vector is determined. This characterizes the optimal complementary index under each timescale as

captured in the proposed approach. As indicated earlier, *w* (wind), *h* (hydro) and *s* (solar) is used as an index to identify each resource.

For this region under study, the data sets for solar irradiation and wind speed correspond to satellite measurements [65]. From past studies, it is worth noting that these datasets have exhibited a solid match [66]. Figure 7 displays the data maps depicting the trends of the two resources throughout the year on an hourly average schedule based on the capacity factor.

4.1. Early Evidence of Complementarity

Figure 9 illustrates a matrix for 8760 h at a 24-h 365-day resolution that reflects daily variation in the efficacy of wind and solar output generation while Figure 10 presents the average daily and seasonal trends in wind and solar power generation. The graph shows that wind power generation tends to be slightly higher in the evening and throughout the night than in the morning. In comparison, solar power exhibits less sub-daily variability. However, the seasonality of wind power generation is significantly more pronounced as compared to solar power. Throughout the year, solar power output is generally constant, with slightly lower values during the rainy season that can be attributed to an increase in fogginess [67,68].

Wind power demonstrates a bi-modal seasonality, characterized by two distinct peaks. The first peak occurs in January, while the second peak is observed between September and November. On the other hand, when considering inter-annual variability, Figure 10 indicates that wind energy exhibits significantly higher variability compared to solar PV. This suggests that wind power generation is subject to greater year-to-year fluctuations than solar power generation in the studied region.

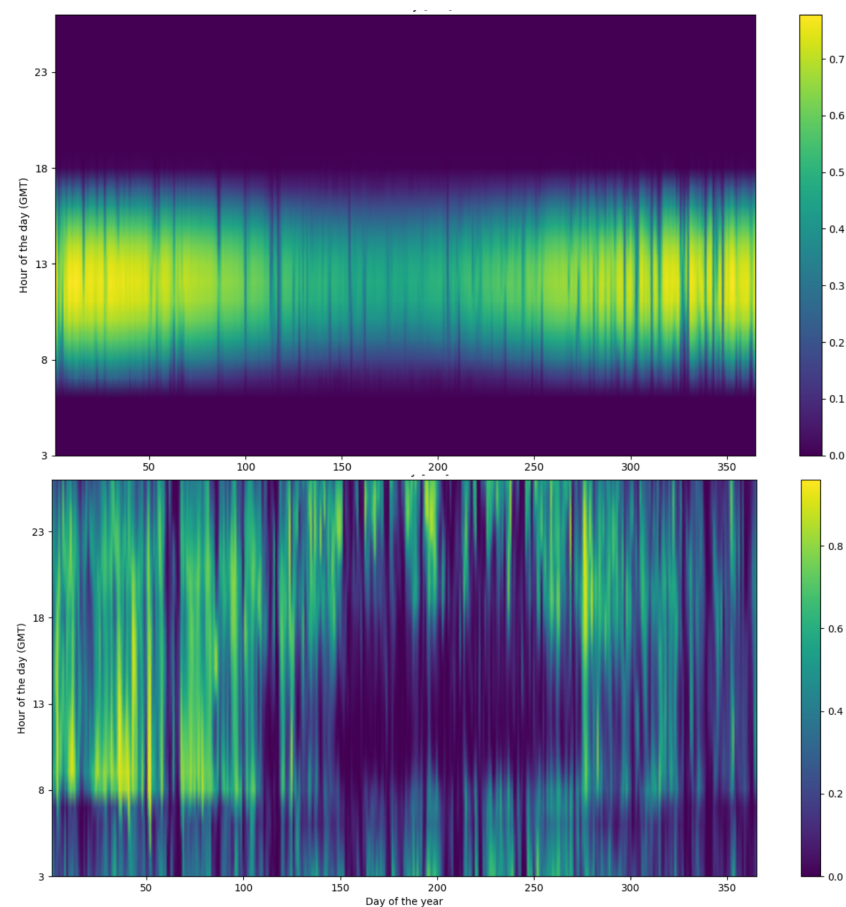


Figure 9. Normalised performance of wind (bottom) and solar PV diurnal power generation capability.

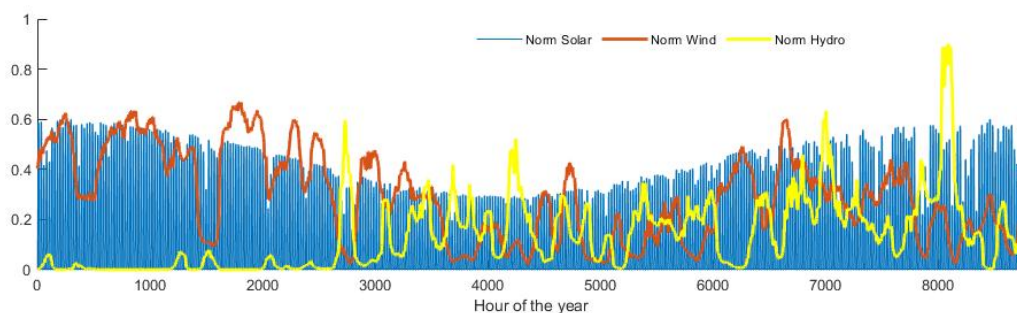


Figure 10. Normalised time series for hourly resource.

4.2. Analysis of W-H-S Complementary Characteristics on Annual Scale

Complementarity assessments between the three energy sources were based on capacity factors on an hourly time-step. To calculate wind and solar PV capacity factors, hourly climatology data are first obtained from the Modern-Era Retrospective Analysis for Research and Application Version 2 (MERRA-2) that has a horizontal resolution of 0.5° (latitude) and 0.625° (longitude) with 2019 as the base year [56].

Table 2 and Figure 11 details the results for energetic complementarity, computed on an annual time scale. These results indicate that among the three paired combinations, the annual complementarity of wind and hydro resources is highest, indicating that months with lower average wind speeds typically have higher average precipitation and vice versa. This is consistent with the findings of Funk et al. [69]. Generally, the onset of Kenya's two wet seasons is often signaled by the winds. The first season, known as the hot northeast monsoon (kaskazi), brings dry air from the Persian Gulf, and lasts from November to March/April. The humid and warm kusi monsoon in the second spell blows from the southeast between May and October.

Similarly, the paired combination of solar and hydro presents a strong complementarity ($\tau_{sh} = -0.123$) while solar and wind exhibits moderate complementarity ($\tau_{ws} = -0.065$), suggesting that the paired resources follow dissimilar patterns in terms of their relative variability across the year.

Table 2. The complementary characteristics of the reference case based on yearly data.

Kendall Tau Correlation Coefficient—(τ_{xy})	
Complementarity vector	$-0.065ws - 0.198wh - 0.123sh$
Compromise programming	1.307
Total temporal complementarity index— κ_t	75.24%

As per the attained complementary index, W-H-S exhibit significant complementary attributes. This means correlation between the three sources has a big impact on the overall complementary index at an annual scale. Based on these results, a month-ahead or season-long scheduling system operation would in all likelihood achieve improved performance by utilizing a compromised mix of all three sources.

4.3. Complementary Characteristics of W-H-S on Monthly Timescale

The wind, solar, and hydropower output data over 12 months with 2019 as the base year are used for complementarity computation and analysis. The findings are summarized in Table 3 and Figures 12–15, showing the contribution of each pair of resources to the overall complementarity index.

Observations point to an outrageous contrast on the complementary attributes during certain months of the year. There is strong complementarity between June and September, medium complementarity in March, April, May, October through to December and finally weak complementarity in January and February.

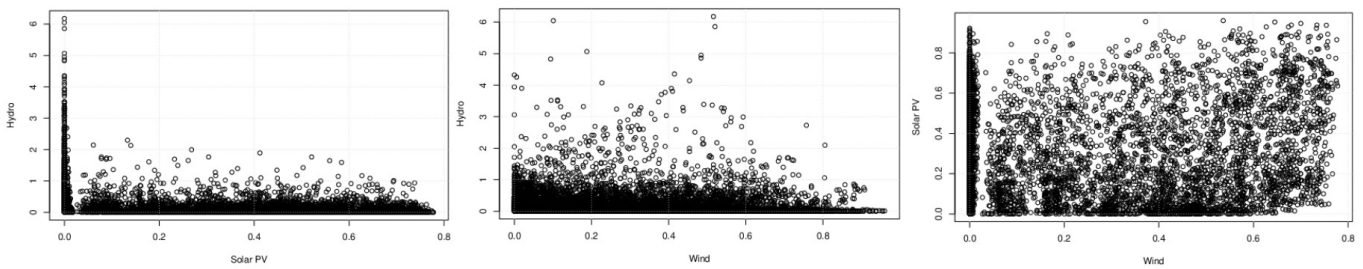


Figure 11. Scatterplot showing annual hourly variation for the paired power resources.

From the results on a monthly timescale, complementarity index k_t ranges from 60.74 in January up to 81.33% in June. In the context of Table 3, it can be argued that there is a moderate-to-strong bundle complementarity based on the joint behavior of the three energy sources on a monthly period. The graph in Figure 12 shows the contribution of each pairwise combination on k_t , based on the normalised individual distances computed using the adopted algorithm. From the results shown, it is observed that solar–hydro pair of resources offers a substantial contribution to the overall complementarity across the year on a monthly time scale. Wind–solar too has a great match from May to October while wind–hydro in January to April and in December.

Table 3. Complementarity results on a monthly scale for the reference case.

Month	Complementary Vector c	Spatial Optimal Solution, $L(c)$	Total Complementary Index, $k_t(c)$
1	$0.261ws - 0.009wh - 0.029sh$	1.611	61.74
2	$0.233ws - 0.142wh - 0.020sh$	1.536	65.08
3	$0.244ws - 0.343wh - 0.106sh$	1.398	71.20
4	$0.027ws - 0.249wh - 0.212sh$	1.283	76.31
5	$-0.357ws + 0.021wh - 0.061sh$	1.302	75.47
6	$-0.481ws + 0.030wh - 0.209sh$	1.170	81.33
7	$-0.400ws + 0.080wh - 0.182sh$	1.249	77.84
8	$-0.381ws + 0.016wh - 0.210sh$	1.213	79.44
9	$-0.441ws - 0.151wh - 0.057sh$	1.175	81.10
10	$-0.151ws + 0.135wh - 0.097sh$	1.443	69.19
11	$0.011ws + 0.084wh - 0.278sh$	1.408	70.76
12	$0.087ws - 0.166wh - 0.155sh$	1.383	71.87

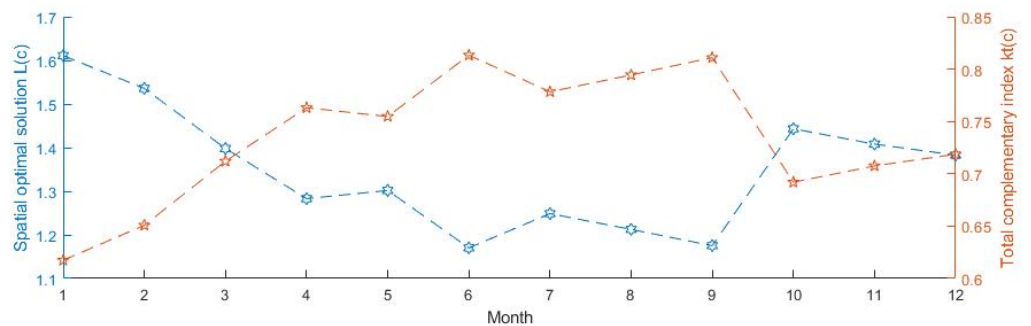


Figure 12. Monthly variation of the complementary index.

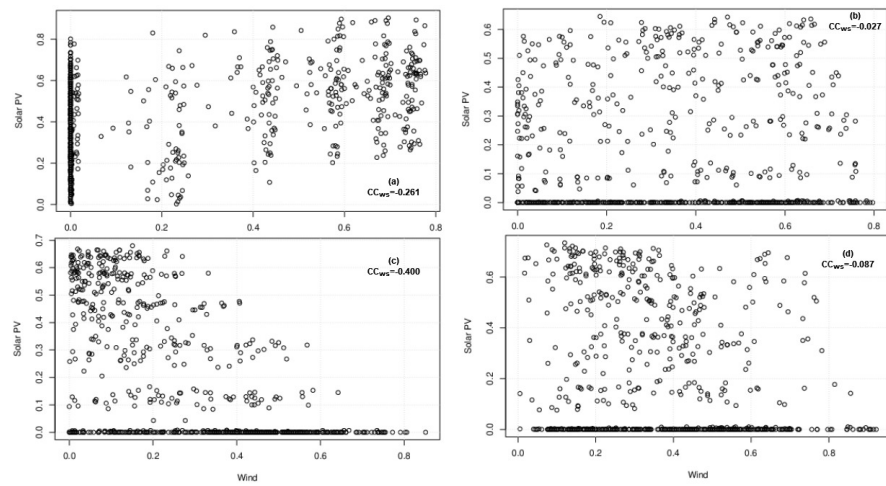


Figure 13. Scatterplot showing the monthly correlation of the wind and solar PV power resource for (a) January, (b) April, (c) July and (d) October.

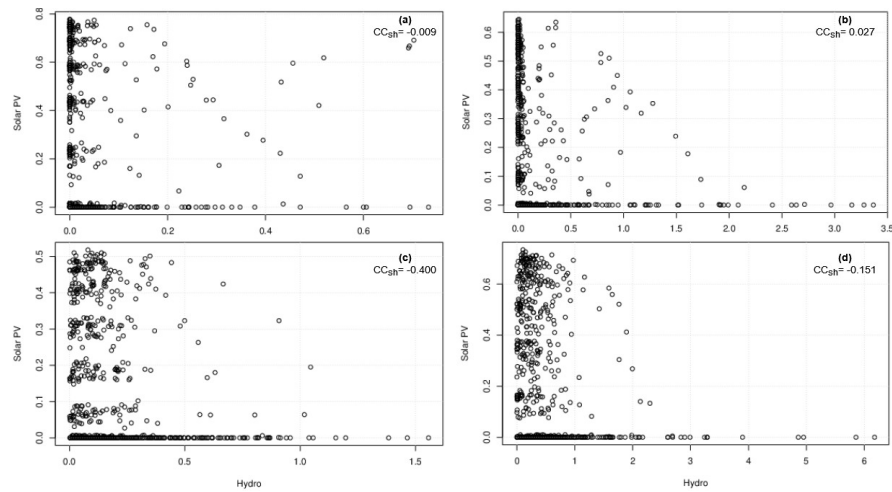


Figure 14. Scatterplot showing the monthly correlation of the solar PV and hydropower resource for: (a) January, (b) April, (c) July and (d) October.

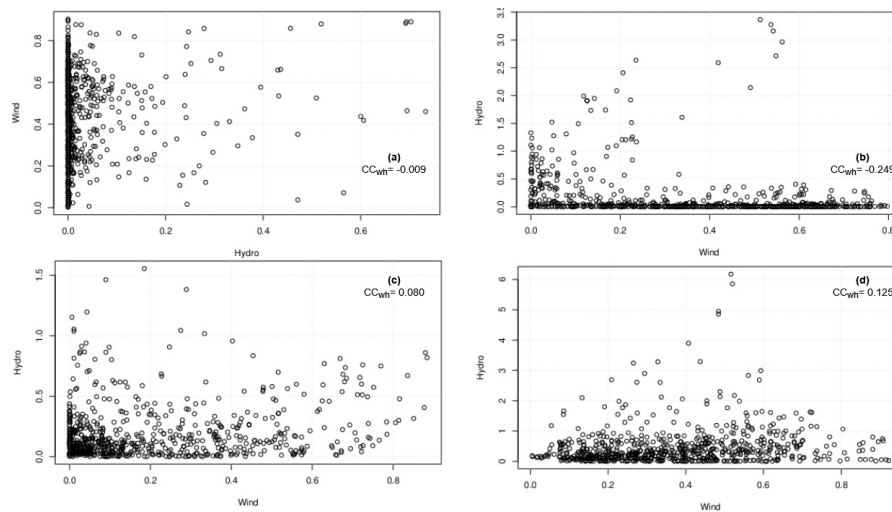


Figure 15. Scatterplot showing the monthly correlation of the wind and hydropower resource for: (a) January, (b) April, (c) July and (d) October.

4.4. Complementary Characteristics of W-H-S on Daily Scale

By examining the normalized time series of the average hourly resources depicted in Figure 10, it becomes evident that there is a noticeable synergy between wind and solar output power generation. Additionally, the wind and hydro resources exhibit some similarities on a diurnal scale. This is further supported by the results presented in Table 4, which indicate that the individual correlations lie within weak-to-moderate complementary range, which indicate that the individual correlations range from weak-to-moderate complementarity. These findings highlight the potential stability strengths of employing W-H-S resources in the region.

Table 4. Complementarity results on a daily scale for the reference case.

Day of Month	Complementary Vector c	Spatial Optimal Solution, $L(c)$	Total Complementary Index, $k_t(c)$
1/1	$0.519ws + 0.369wh + 0.758sh$	2.323	30.08%
2/1	$0.190ws + 0.500wh + 0.800sh$	2.245	33.55%
3/1	$0.304ws + 0.319wh + 0.115sh$	1.869	50.27%
4/1	$0.053ws - 0.128wh - 0.563sh$	1.181	80.85%
5/1	$-0.023ws + 0.394wh - 0.239sh$	1.567	63.71%
6/1	$-0.407ws + 0.581wh - 0.385sh$	1.395	71.34%
7/1	$-0.781ws + 0.083wh - 0.081sh$	1.110	83.98%
8/1	$-0.320ws + 0.252wh - 0.247sh$	1.342	73.67%
9/1	$0.123ws + 0.303wh - 0.538sh$	1.444	69.17%
10/1	$0.146ws + 0.412wh + 0.093sh$	1.826	52.20%
11/1	$-0.814ws + 0.507wh - 0.481sh$	1.106	84.19%
12/1	$0.566ws - 0.567wh - 0.753sh$	1.124	83.40%

However, a proper combination of the three resources in a hybrid power setup may result in better performance for this timescale, as connoted by the results for k_t . A combination of any of the two, would possibly necessitate a significant incorporation of energy storage or backup power. The scatter plots in Figure 16 shows the contribution of each paired set of resources to the overall complementarity, k_t . It is worth noting that wind–hydro and wind–solar resources offer comparably fair share towards the k_t value, implying that any meaningful planning and day-to-day operation of hybrid system should utilize wind power as the primary energy source, complemented by other two sources.

The diurnal cycle as expected has a significant impact on wind–solar complementarity as noted by Jurasz et al. [70] This yields almost zero linear relationship between these two resources especially between January and April resulting in very weak complementarity. The other paired combinations also envisage varying complementarity across the year.

However, considering a trio bundle of the resources together, the overall temporal complementarity on a diurnal scale yields different k_t values, ranging from 30.08% to 84.19% as the feasible maximum. A combination of these three resources in a hybrid power setup may lead to better results for this timescale, as connoted by the results for k_t except for the first three months. A combination of wind and solar resources would likely require a substantial amount of energy storage or backup power to ensure reliable electricity supply. The scatter plot depicted in Figure 16 illustrates the contribution of each pair combination to the complementarity index k_t . It is noteworthy that the combination of solar and hydro resources, as well as wind and solar resources positively affects the value of k_t . This suggests that in the case of daily-scale system planning and operation, solar power should be considered as the primary energy source, complemented by the other two sources. This finding emphasizes the importance of incorporating solar power into the energy mix to enhance complementarity and optimize system performance.

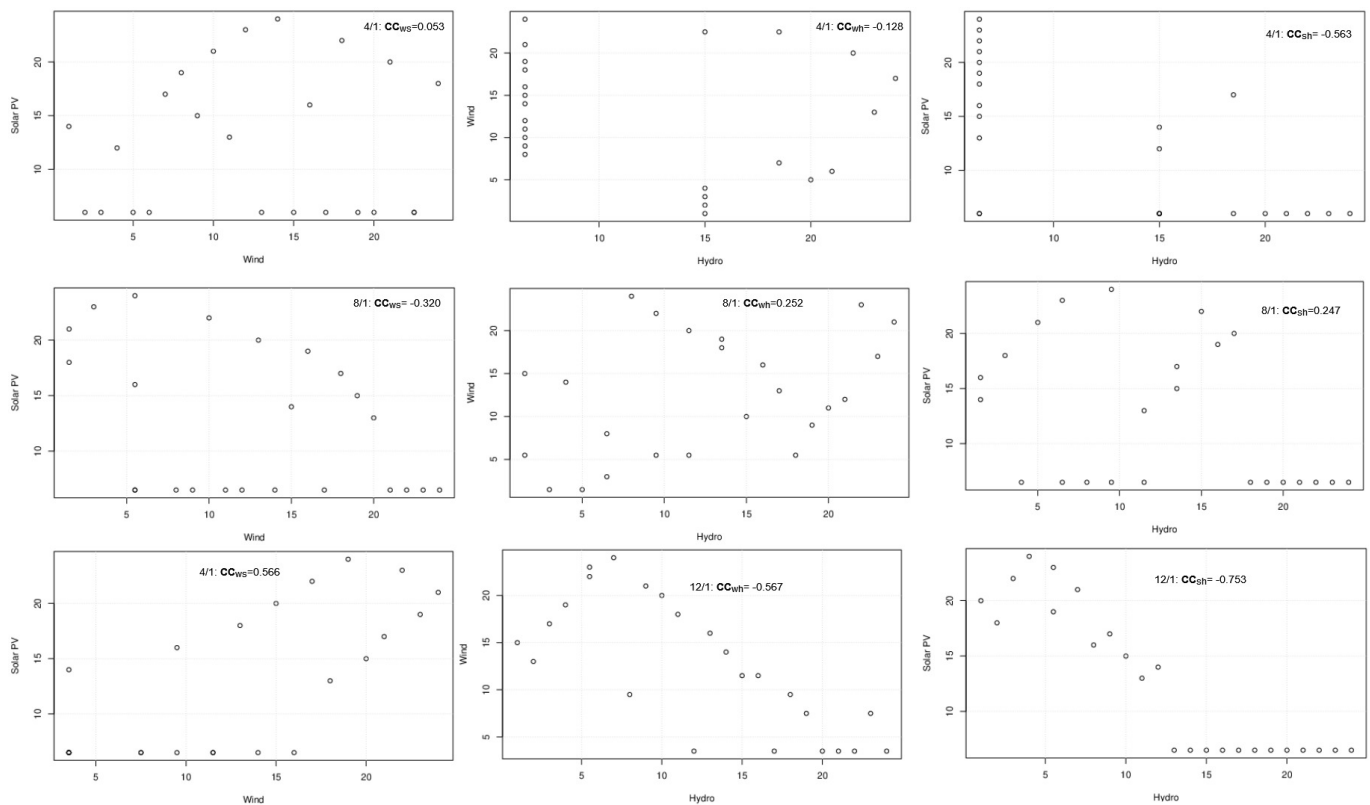


Figure 16. Scatterplot showing the diurnal variation of each paired source.

4.5. Temporo-Spatial Congruity between Wind/Solar and Hydropower Resources

Technically, grid integration of VRE resources requires a significant level of flexible and controllable power supply, especially to balance and avoid outages during daily peak hours. However, the variability of wind and solar output power can effectively be mitigated via complementarity and appropriate capacity mix. Therefore, when regulated well, integrating hydro, wind and solar energy into a hybrid energy system is an effective way to increase grid penetration of VRE sources [45].

Hydropower as the baseline is utilized to regulate the intermittency of wind and solar photovoltaic power in the *w-h-s* hybrid energy system, which effectively boosts energy utilization. The study provides a framework to determine the optimal installed capacity configuration by considering power supply characteristics besides the uptake. The k_{stab} encompasses a two-stage adaptive complementary metric which demonstrates the ability of the wind–solar to augment hydropower in meeting the projected power balance with each VRE source contributing a fair share.

Figure 17 shows the share apportioned to either wind or solar as the VRE is increased from 5% to 50%. As observed, wind power carries slightly more weight, 8 points more than solar to attain a better output configurations that enjoys more output absorption as well as levelise output fluctuations. With 5% VRE share contribution, wind produces 54.03% while solar accounts for the difference. As the contribution of the VRE increase to 50%, the share of wind portion in the VRE slightly increases to 47.41%.

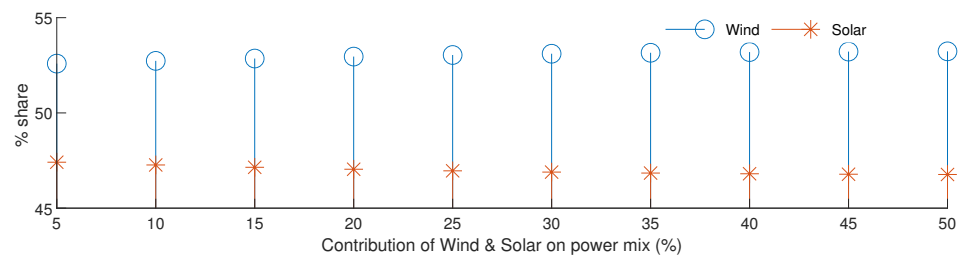


Figure 17. Annual wind and solar power generation pattern.

Histogram plots in Figure 18 shows the distribution of solar, wind power and combined output from the two sources on hourly basis across the year. Based on extensive resource assessments, it is evident that the region possesses a consistently high wind potential throughout the year, ensuring reliable generation capabilities [71]. Figure 18 presents a weighted average of the capacity factors for both wind and solar PV in Kenya, showcasing the remarkable synergy between these two renewable energy sources. This shows that a higher proportion of wind energy in the power mix yields better feasibility [59].

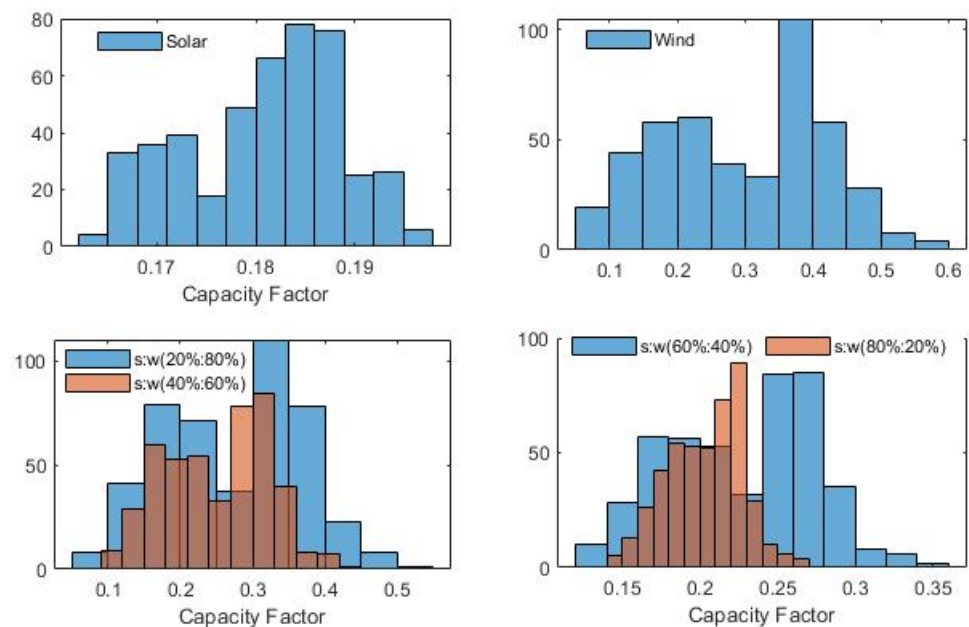


Figure 18. Histogram plots showing the distribution of solar power, wind power and combined production on hourly basis across the year.

As can be noted, Kenya has abundant solar and wind resources, with fairly strong complementarity. Furthermore, the availability of hydro resources and the region's splendid geographical conditions provide requisite essentials for large-scale integration of wind and solar energy. In addition, configuring the right power profile can further improve system flexibility to better adapt to wind and solar energy. This is of great importance to system planners.

5. Conclusions

The challenges of accommodating renewables into the existing energy mix tend to increase as the share of VRE increases. And yet, regions are quite diverse, hence challenges and related measures are dependent on many other characteristics. This means that power sector transition should be approached in a multi-dimensional manner.

Planning for VRE sources with a “smoother” power output generation is indeed a worthwhile course of harnessing and maximizing the integration of renewable energy into

existing energy systems. The proposed metric allows assessing complementarity between existing hydro-dominant systems and other available variable renewable energy sources such as wind and solar. It also suggests potential modifications to the system's operation that leverage the temporal complementarity of these energy sources smoothing its load following capability through optimal power mixes. Therefore, this study puts forward the following suggestions for power system planners and policy makers in this region:

1. As the local electricity load demand continues to grow steadily, it is imperative to explore additional renewable energy options to meet this demand.
2. The complementarity of VRE sources in the region is comparatively good, therefore, on appraising the power system flexibility in the region, it should be given utmost consideration when planning new power plants.

The extent of complementarity, its features, and the room for its enhancement are predominantly influenced by local conditions. In order to gain deeper insights, the authors of this study plan to conduct further investigations that consider the spatial aspects. Future analyses will explore potential strategies for reducing intermittency by exploring adjustments in the placement of the wind and PV systems. This exploration aims to identify optimal locations that can enhance complementarity within hydro-dominated systems.

However, the incorporation of storage facilities and other system restrictions (such as the capacity of backup sources) in our modeling framework would be an important extension of our work. Nevertheless, this analysis offers a critical evaluation of the potential contribution that VRES complementarity brings towards a smooth transition to renewable energy.

Author Contributions: D.J. conducted a literature survey, collected and processed the data, implemented necessary computational routines and wrote the manuscript. J.M. and C.K. edited and reviewed the manuscript alongside supervision. All authors have read and agreed to the published version of the manuscript.

Funding: This research is partially funded by the African Center of Excellence in Energy for Sustainable Development, University of Rwanda (Research Core Funding No. ACE II-017).

Data Availability Statement: Publicly available datasets were analysed in this study; accessible online: <https://www.renewables.ninja/>.

Conflicts of Interest: The authors declare no conflicts of interest.

Abbreviations

CC	Correlation Coefficients
CF	Capacity Factor
CSP	Concentrated Solar Power
GHG	Global Greenhouse Gas
GHI	Global Horizontal Irradiation
PV	Photovoltaic
RE	Renewable Energy
RE	Renewable Energy Sources
VRE	Variable Renewable Energy

References

1. Teske, S.; Giurco, D.; Morris, T.; Nagrath, K.; Mey, F.; Briggs, C.; Dominish, E.; Florin, N. *Achieving the Paris Climate Agreement Goals: Global and Regional 100% Renewable Energy Scenarios to Achieve the Paris Agreement Goals with Non-Energy GHG Pathways for +1.5 °C and +2 °C*; Springer: Cham, Switzerland, 2019.
2. Hirpa, F.A.; Dyer, E.; Hope, R.; Olago, D.O.; Dadson, S.J. Finding sustainable water futures in data-sparse regions under climate change: Insights from the Turkwel River basin, Kenya. *J. Hydrol. Reg. Stud.* **2018**, *19*, 124–135. [CrossRef]
3. Hall, S. Power-Sector Emissions Are Set to Fall in 2022. Thanks to Renewable Energy. 2022. Available online: <https://climatechampions.unfccc.int/power-sector-emissions-are-set-to-fall-in-2022-thanks-to-renewable-energy/> (accessed on 20 October 2022).

4. Bogdanov, D.; Ram, M.; Aghahosseini, A.; Gulagi, A.; Oyewo, A.S.; Child, M.; Caldera, U.; Sadovskaia, K.; Farfan, J.; De Souza Noel Simas Barbosa, L.; et al. Low-cost renewable electricity as the key driver of the global energy transition towards sustainability. *Energy* **2021**, *227*, 120467. [CrossRef]
5. Cheng, Q.; Liu, P.; Xia, J.; Ming, B.; Cheng, L.; Chen, J.; Xie, K.; Liu, Z.; Li, X. Contribution of complementary operation in adapting to climate change impacts on a large-scale wind-solar-hydro system: A case study in the Yalong River Basin, China. *Appl. Energy* **2022**, *325*, 119809. [CrossRef]
6. Hunt, T. Has the International Energy Agency Finally Improved at Forecasting Solar Growth? 2020. Available online: <https://pv-magazine-usa.com/2020/07/12/has-the-international-energy-agency-finally-improved-at-forecasting-solar-growth/> (accessed on 19 October 2022).
7. Namahoro, J.P.; Wu, Q.; Xiao, H.; Zhou, N. The Impact of Renewable Energy, Economic and Population Growth on CO₂ Emissions in the East African Region: Evidence from Common Correlated Effect Means Group and Asymmetric Analysis. *Energies* **2021**, *14*, 312. [CrossRef]
8. Falchetta, G.; Gernaat, D.E.; Hunt, J.; Sterl, S. Hydropower dependency and climate change in sub-Saharan Africa: A nexus framework and evidence-based review. *J. Clean. Prod.* **2019**, *231*, 1399–1417. [CrossRef]
9. Falchetta, G.; Pachauri, S.; Byers, E.; Danylo, O.; Parkinson, S.C. Satellite Observations Reveal Inequalities in the Progress and Effectiveness of Recent Electrification in Sub-Saharan Africa. *One Earth* **2020**, *2*, 364–379. [CrossRef]
10. Oyewo, A.S.; Aghahosseini, A.; Ram, M.; Breyer, C. Transitions towards decarbonised power systems and its socio-economic impacts in West Africa. *Renew. Energy* **2020**, *154*, 1092–1112. [CrossRef]
11. Alova, G.; Trotter, P.A.; Money, A. A machine-learning approach to predicting Africa’s electricity mix based on planned power plants and their chances of success. *Nat. Energy* **2021**, *6*, 158–166. [CrossRef]
12. Sterl, S. A Grid for all Seasons: Enhancing the Integration of Variable Solar and Wind Power in Electricity Systems Across Africa. *Curr. Sustain. Energy Rep.* **2021**, *8*, 274–281. [CrossRef]
13. Maulidi, B.; Dmitrii, B.; Solomon, O.A.; Christian, B. A cost optimal resolution for Sub-Saharan Africa powered by 100% renewables in 2030. *Renew. Sustain. Energy Rev.* **2018**, *92*, 440–457.
14. IRENA. Planning and Prospects for Renewable Power: Eastern and Southern Africa, 2021. Available online: <https://www.irena.org/publications/2021/Apr/Planning-and-prospects-for-renewable-power-Eastern-and-Southern-Africa> (accessed on 20 October 2022).
15. Wu, G.C.; Deshmukh, R.; Ndhlukula, K.; Radojicic, T.; Reilly-Moman, J.; Phadke, A.; Kammen, D.M.; Callaway, D.S. Strategic siting and regional grid interconnections key to low-carbon futures in African countries. *Proc. Natl. Acad. Sci. USA* **2017**, *114*, E3004–E3012. [CrossRef]
16. Aghahosseini, A.; Bogdanov, D.; Breyer, C. Towards sustainable development in the MENA region: Analysing the feasibility of a 100% renewable electricity system in 2030. *Energy Strategy Rev.* **2020**, *28*, 100466. [CrossRef]
17. Jurasz, J.; Canales, F.; Kies, A.; Guezgouz, M.; Beluco, A. A review on the complementarity of renewable energy sources: Concept, metrics, application and future research directions. *Sol. Energy* **2020**, *195*, 703–724. [CrossRef]
18. Solomon, O.; Asfaw, S.; Bogdanov, D.; Aghahosseini, A.; Mensah, T.; Ram, M. Just transition towards defossilised energy systems for developing economies: A case study of Ethiopia. *Renew. Energy* **2021**, *176*, 346–365. [CrossRef]
19. Bogdanov, D.; Aghahosseini, A.; Gulagi, A.; Child, M.; Solomon, O.; Farfan Orozco, F.; Sadovskaia, K.; Vainikka, P. Solar photovoltaics demand for the global energy transition in the power sector. *Prog. Photovoltaics Res. Appl.* **2018**, *25*, 523. [CrossRef]
20. Elkadeem, M.R.; Younes, A.; Sharshir, S.W.; Campana, P.; Wang, S. Sustainable siting and design optimization of hybrid renewable energy system: A geospatial multi-criteria analysis. *Appl. Energy* **2021**, *295*, 117071. [CrossRef]
21. Sterl, S.; Fadly, D.; Liersch, S.; Koch, H.; Thiery, W. Linking solar and wind power in eastern Africa with operation of the Grand Ethiopian Renaissance Dam. *Nature Energy* **2021**, *6*, 407–418. [CrossRef]
22. Timmons, D.; Dhunny, A.; Elahee, K.; Havumaki, B.; Howells, M.; Khoodaruth, A.; Lema-Driscoll, A.; Lollchund, M.; Ramgolam, Y.; Rughooputh, S.; et al. Cost minimization for fully renewable electricity systems: A Mauritius case study. *Energy Policy* **2019**, *133*, 110895. [CrossRef]
23. Oyewo, A.S.; Sterl, S.; Khalili, S.; Breyer, C. Highly renewable energy systems in Africa: Rationale, research, and recommendations. *Joule* **2023**, *7*, 1437–1470. [CrossRef]
24. Nyenah, E.; Sterl, S.; Thiery, W. Pieces of a puzzle: Solar-wind power synergies on seasonal and diurnal timescales tend to be excellent worldwide. *Environ. Res. Commun.* **2022**, *4*, 055011. [CrossRef]
25. Sterl, S.; Liersch, S.; Koch, H.; van Lipzig, N.P.; Thiery, W. A new approach for assessing synergies of solar and wind power: implications for West Africa. *Environ. Res. Lett.* **2018**, *13*, 094009. [CrossRef]
26. Škrbić, B.; Đurišić, Ž. Novel Planning Methodology for Spatially Optimized RES Development Which Minimizes Flexibility Requirements for Their Integration into the Power System. *Energies* **2023**, *16*, 3251. [CrossRef]
27. Scott, I.J.; Carvalho, P.M.; Botterud, A.; Silva, C.A. Clustering representative days for power systems generation expansion planning: Capturing the effects of variable renewables and energy storage. *Appl. Energy* **2019**, *253*, 113603. [CrossRef]
28. Geem, Z.W.; Kim, J.H. Optimal Energy Mix with Renewable Portfolio Standards in Korea. *Sustainability* **2016**, *8*, 423. [CrossRef]
29. Cho, S.; Kim, H.; Lee, S.; Kim, S.; Jeon, E.C. Optimal energy mix for greenhouse gas reduction with renewable energy—The case of the South Korean electricity sector. *Energy Env.* **2020**, *31*, 1055–1076. [CrossRef]

30. Huang, M.C.; Kim, C.J. Investigating Cost-Effective Policy Incentives for Renewable Energy in Japan: A Recursive CGE Approach for an Optimal Energy Mix. *Singap. Econ. Rev.* **2020**, *66*, 507–528. [CrossRef]
31. Babonneau, F.; Barrera, J.; Toledo, J. Decarbonizing the Chilean Electric Power System: A Prospective Analysis of Alternative Carbon Emissions Policies. *Energies* **2021**, *14*, 4768. [CrossRef]
32. Hussain, S.; Lai, C.; Eicker, U. Flexibility: Literature review on concepts, modeling, and provision method in smart grid. *Sustain. Energy Grids Netw.* **2023**, *35*, 101113. [CrossRef]
33. Dong, J.; Chen, Z.; Dou, X. The Influence of Multiple Types of Flexible Resources on the Flexibility of Power System in Northwest China. *Sustainability* **2022**, *14*, 11617. [CrossRef]
34. Wessa, P. *Kendall tau Rank Correlation (v1.0.13) in Free Statistics Software (v1.2.1)*; Office for Research Development and Education: 2017. Available online: https://www.wessa.net/rwasp_kendall.wasp/ (accessed on 6 September 2023).
35. Kendall, M.G. A new measure of rank correlation. *Biometrika* **1938**, *30*, 81–93. [CrossRef]
36. Kendall tau Metric—Encyclopedia of Mathematics. 2023. Available online: https://encyclopediaofmath.org/wiki/Kendall_tau_metric (accessed on 6 September 2023).
37. Canales, F.; Jurasz, J.; Beluco, A.; Kies, A. Assessing temporal complementarity between three variable energy sources through correlation and compromise programming. *Energy* **2019**, *192*, 116637. [CrossRef]
38. Sharma, P.; Said, Z.; Kumar, A.; Nizetic, S.; Pandey, A.; Hoang, A.; Huang, Z.; Afzal, A.; Li, C.; Le Anh, T.; et al. Recent Advances in Machine Learning Research for Nanofluid-Based Heat Transfer in Renewable Energy System. *Energy Fuels* **2022**, *36*, 6626–6658. [CrossRef]
39. Gershon, M.; Duckstein, L. Multiobjective Approaches to River Basin Planning. *J. Water Resour. Plan. Manag.* **1981**, *109*, 13–28. [CrossRef]
40. Wang, S.; Jia, R.; Luo, C.; An, Y.; Guo, P. Spatiotemporal Complementary Characteristics of Large-Scale Wind Power, Photovoltaic Power, and Hydropower. *Sustainability* **2022**, *14*, 9273. [CrossRef]
41. Liu, Y.; Xiao, L.; Wang, H.; Dai, S.; Qi, Z. Analysis on the hourly spatiotemporal complementarities between China’s solar and wind energy resources spreading in a wide area. *Sci. China Technol. Sci.* **2013**, *56*, 683–692. [CrossRef]
42. Francois, B.; Borga, M.; Creutin, J.; Hingray, B.; Raynaud, D.; Sauterleute, J. Complementarity between solar and hydro power: Sensitivity study to climate characteristics in Northern-Italy. *Renew. Energy* **2016**, *86*, 543–553. [CrossRef]
43. Gils, H.; Scholz, Y.; Pregger, T.; Luca de Tena, D.; Heide, D. Integrated modelling of variable renewable energy-based power supply in Europe. *Energy* **2017**, *123*, 173–188. [CrossRef]
44. do Couto, A.F.; Estanqueiro, A. Exploring Wind and Solar PV Generation Complementarity to Meet Electricity Demand. *Energies* **2020**, *13*, 4132. [CrossRef]
45. Ma, T.; Yang, H.; Lu, L. Optimal design of an autonomous solar–wind–pumped storage power supply system. *Appl. Energy* **2014**, *160*, 728–736. [CrossRef]
46. Couto, A.; Estanqueiro, A. Assessment of wind and solar PV local complementarity for the hybridization of the wind power plants installed in Portugal. *J. Clean. Prod.* **2021**, *319*, 128728. [CrossRef]
47. Huang, Y.; Chen, A.; Liu, T.; Wang, W.S. Assessment and Configuration of the Wind-PV-wave Complementary System for Improving the Stability and Power Generation Ability. In Proceedings of the 2022 4th International Conference on Smart Power & Internet Energy Systems (SPIES), Beijing, China, 9–12 December 2022; pp. 1344–1349.
48. Cantor, D.; Ochoa, A.; Mesa, O. Total Variation-Based Metrics for Assessing Complementarity in Energy Resources Time Series. *Sustainability* **2022**, *14*, 8514. [CrossRef]
49. Iwueze, I.; Nwogu, E.; Nlebedim, V.; Imoh, J. Comparison of Two Time Series Decomposition Methods: Least Squares and Buys-Ballot Methods. *Open J. Stat.* **2016**, *6*, 1123–1137. [CrossRef]
50. Francois, B.; Martino, S.; Tofte, L.; Hingray, B.; Mo, B.; Creutin, J. Effects of Increased Wind Power Generation on Mid-Norway’s Energy Balance under Climate Change: A Market Based Approach. *Energies* **2017**, *10*, 227. [CrossRef]
51. McPherson, M.; Sotiropoulos-Michalakakos, T.; Harvey, L.D.; Karney, B. An Open-Access Web-Based Tool to Access Global, Hourly Wind and Solar PV Generation Time-Series Derived from the MERRA Reanalysis Dataset. *Energies* **2017**, *10*, 1007. [CrossRef]
52. Davis, P.J. *Interpolation and Approximation*; Dover Publications: Mineola, NY, USA, 1975.
53. Avery, S. Lake Turkana and the Lower Omo: Hydrological Impacts of Major Dam and Irrigation Developments. 2012. Available online: https://africanstudies.web.ox.ac.uk/sites/default/files/africanstudies/documents/media/executive_summary_introduction.pdf (accessed on 21 October 2022).
54. Takase, M.; Kipkoeh, R.; Essandoh, P.K. A comprehensive review of energy scenario and sustainable energy in Kenya. *Fuel Commun.* **2021**, *7*, 100015. [CrossRef]
55. Staffell, I.; Pfenninger, S. Using bias-corrected reanalysis to simulate current and future wind power output. *Energy* **2016**, *114*, 1224–1239. [CrossRef]
56. Pfenninger, S.; Staffell, I. Long-term patterns of European PV output using 30 years of validated hourly reanalysis and satellite data. *Energy* **2016**, *114*, 1251–1265. [CrossRef]
57. Grams, C.; Beerli, R.; Pfenninger, S.; Staffell, I.; Wernli, H. Balancing Europe’s wind-power output through spatial deployment informed by weather regimes. *Nat. Clim. Chang.* **2017**, *7*, 557–562. [CrossRef]

58. The Largest Wind Power Plant in Africa Has Opened in Kenya, 2023. Available online: <https://www.weforum.org/agenda/2019/07/wind-power-project-opens-in-kenya/> (accessed on 22 April 2023).
59. Bloomfield, H.C.; Wainwright, C.M.; Mitchell, N. Characterizing the variability and meteorological drivers of wind power and solar power generation over Africa. *Meteorol. Appl.* **2022**, *29*, e2093. [[CrossRef](#)]
60. King, J.A.; Engelstaedter, S.; Washington, R.; Munday, C. Variability of the Turkana Low-Level Jet in Reanalysis and Models: Implications for Rainfall. *J. Geophys. Res. Atmos.* **2021**, *126*, e2020JD034154. [[CrossRef](#)]
61. Gong, W.; Liu, P.; Cheng, L.; Li, H.; Yang, Z. A varying comprehensive hydropower coefficient for medium/long-term operation of a single reservoir. *Hydrol. Res.* **2020**, *51*, 686–698. [[CrossRef](#)]
62. Jin, X.; Wu, Q. Local flexibility markets: Literature review on concepts, models and clearing methods. *Appl. Energy* **2020**, *261*, 114387. [[CrossRef](#)]
63. Babatunde, O.; Munda, J.; Hamam, Y. Power system flexibility: A review. *Energy Rep.* **2020**, *6*, 101–106. [[CrossRef](#)]
64. Akrami, A.; Doostizadeh, M.; Aminifar, F. Power system flexibility: An overview of emergence to evolution. *J. Mod. Power Syst. Clean Energy* **2019**, *7*, 987–1007. [[CrossRef](#)]
65. Renewables.ninja. 2022. Available online: <https://www.renewables.ninja/> (accessed on 21 October 2022).
66. Kies, A.; Schyska, B.U.; Bilousova, M.; El Sayed, O.; Jurasz, J.; Stoecker, H. Critical review of renewable generation datasets and their implications for European power system models. *Renew. Sustain. Energy Rev.* **2021**, *152*, 111614. [[CrossRef](#)]
67. Camberlin, P.; Wairoto, J.G. Intraseasonal wind anomalies related to wet and dry spells during the ‘long’ and ‘short’ rainy seasons in Kenya. *Theor. Appl. Climatol.* **1997**, *58*, 57–69. [[CrossRef](#)]
68. Edwards, G.; Dent, C.J.; Wade, N. Assessing the Potential Impact of Grid-Scale Variable Renewable Energy on the Reliability of Electricity Supply in Kenya. *IDS Bull.* **2017**, *48*, 29–48. [[CrossRef](#)]
69. Funk, C.; Hoell, A.; Shukla, S.; Husak, G.; Michaelsen, J. The East African Monsoon System: Seasonal Climatologies and Recent Variations. In *The Monsoons and Climate Change*; Springer: Cham, Switzerland, 2016; pp. 163–185. [[CrossRef](#)]
70. Jurasz, J.; Beluco, A.; Canales, F. The impact of complementarity on power supply reliability of small scale hybrid energy systems. *Energy* **2018**, *161*, 737–743. [[CrossRef](#)]
71. Fant, C.; Gunturu, B.; Schlosser, A. Characterizing wind power resource reliability in southern Africa. *Appl. Energy* **2016**, *161*, 565–573. [[CrossRef](#)]

Disclaimer/Publisher’s Note: The statements, opinions and data contained in all publications are solely those of the individual author(s) and contributor(s) and not of MDPI and/or the editor(s). MDPI and/or the editor(s) disclaim responsibility for any injury to people or property resulting from any ideas, methods, instructions or products referred to in the content.